Available online at www.sciencedirect.com
ScienceDirect
Chinese Journal of Aeronautics 23(2010) 162-169
Chinese Journal of Aeronautics
www.elsevier.com/locate/cja

Large-eddy Simulation of Near-field Dynamics in a Particle-laden Round Turbulent Jet

Wang Bing, Zhang Huiqiang*, Wang Xilin

School of Aerospace, Tsinghua University, Beijing 100084, China

Received 18 March 2009; accepted 15 September 2009

Abstract

This article investigates the near-field dynamics in a particle-laden round turbulent jet in a large-eddy simulation (LES). A point-force two-way coupling model is adopted in the simulation to reveal the particle modulation of turbulence. The particles mainly excite the initial instability of the jet and bring about the earlier breakup of vortex rings in the near-field. The flow fluctuating intensity either in the axial or in the radial directions is hence increased by particles. The article also describes the mean velocity modulated by particles. The changing statistical velocity induced by particle modulation implies the effects of modulation of the local flow structures. This study is expected to be useful to the control of two-phase turbulent jets.

Keywords: large-eddy simulation; particle-laden jet; turbulence structures; jet near-fields; two-way coupling

1. Introduction

As a basic type of flow, the two-phase round turbulent jet has found broad application in the aerospace power and propulsion techniques. The dynamics of large-eddy structures and particle dispersion in turbulence are the fundamental factors exerting influences upon the mixing and the combustion efficiency. The flow evolution of the jet, especially the far-field properties, is commonly determined by the near-field vortical dynamics close to the nozzle exit. This induces the necessity of studying the flow properties in the near-field and the particle dispersion in the jet.

The single-phase jet has long been numerically investigated by researchers. R. Verzicco, et al.[1], who studied the vortex dynamics in the jets with low Reynolds numbers of 500 and 1 000, disclosed the statistical features of time-averaged velocities and the variations of momentum layer thickness. Y. Dai, et al.[2] numerically studied a jet in a large-eddy simulation (LES). M. Olsson, et al.[3] pointed out that the statistical data of root mean square fluctuating velocity in the section at $z/D = 6.5$ are smaller than those at $z/D = 7.75$. Q. L. Fan, et al.[4-5] simulated a round turbulent jet in LES, presented the unsteady evolution of the coherent structures and predicted the averaged jet core. However, these investigations are limited to supplying the information about the particle-free turbulent jet only.

S. Yuu, et al.[6] used the direct numerical simulation (DNS) to study a gas-solid jet with a Reynolds number $Re = 1\ 700$, which was laden with 58 μm particles and assumed the particle mass loading ratio to be 0.6. The results they obtained in terms of mean velocity, turbulence intensity as well as Reynolds stress were in good agreement with the measured data by the laser Doppler analyzer (LDA). They unveiled that the on-going turbulence is suppressed by the additional dissipation of turbulence induced by particles. Further, they studied a planar turbulent jet with $Re = 10\ 000$ laden with 65 and 310 μm particles in an LES coupled with a particle trajectory model[7]. They found that the turbulence is checked by particles except in the initial and transition regions, where, in contrast, it is enhanced by larger particles due to large slips between two phases and larger local gradient of particle concentration. K. Luo, et al[8]. studied the effects of particles on two-phase planar jets and found that particles with different Stokes numbers have different influences on the jet. The particles of Stokes numbers 0.01 and 50 accelerate the evolution of flow field and make the curves of gas-phase intensity flatter and wider at different flow sections; but with the particles of Stokes number 1, the exact reverse is the case. Y. Rong[9] es-

*Corresponding author. Tel.: +86-10-62772112-801.
E-mail address: zhanghq@thu.edu.cn
Foundation items: National Natural Science Foundation of China (50706021); Ph.D. Programs Foundation of Ministry of Education of China (20070003018); TNList Cross- discipline Foundation.

doi: 10.1016/S1000-9361(09)60200-4

pecially studied the far-field turbulence modulation in a two-way coupling LES with a spatially developed gas-particle round jet. The predicted data on the turbulence modulated by large and small particles quite agree with the results from the experiments. Nevertheless, little information has been acquired on the near-field behavior of particle dispersion in the flow structures and the modulation with help of particles.

This article mimics a round turbulent particle-laden jet flow by means of an LES associated with a Lagrangian particle trajectory model in cylindrical coordinates. To study the particle dispersion in turbulent structures, a particle is regarded as a mass point and the two-way coupling terms are added into the gas-phase governing equations with the classic point-force model. Particles's inter-collisions are not taken into account under the assumption of the dilute flow. A comparison is made between two-phase instantaneous flow fields together with two-phase statistical results so as to show the effects of particles on the evolution of near-field flows laden with particles.

2. Computation Methods

2.1. Gas-phase equations and discretization methods

The calculation of a round jet flow is performed in cylindrical coordinates. For the convenience of treating the singularity at the axis, variables are transformed into the primitive variables through

$$q_r = r\, v_r,\ q_\theta = v_\theta,\ q_z = v_z\,.$$

where r is the radius and v the velocity.

Applying the box filter to the Navier-Stokes equations and non-dimensioning it by using the nozzle diameter D and the central axial line velocity at the nozzle exit U_{jc} as the reference variables, are obtained the governing equations in an LES as follows:

$$\frac{\partial \overline{q_r}}{\partial r}+\frac{\partial \overline{q_\theta}}{\partial \theta}+r\frac{\partial \overline{q_z}}{\partial z}=0 \tag{1}$$

$$\frac{\partial \overline{q_r}}{\partial t}+\frac{\partial}{\partial r}\left(\frac{\overline{q_r q_r}}{r}\right)+\frac{\partial}{\partial \theta}\left(\frac{\overline{q_r q_\theta}}{r}\right)+\frac{\partial \overline{q_r q_z}}{\partial z}-\overline{q_\theta q_\theta}=$$
$$-r\frac{\partial \overline{p}}{\partial r}+\frac{1}{Re}\left(\frac{\partial r\overline{\tau_{rr}}}{\partial r}+\frac{\partial \overline{\tau_{r\theta}}}{\partial \theta}+r\frac{\partial \overline{\tau_{rz}}}{\partial z}-\overline{\tau_{\theta\theta}}\right) \tag{2}$$

$$\frac{\partial \overline{q_\theta}}{\partial t}+\frac{1}{r^2}\frac{\partial r\overline{q_\theta q_r}}{\partial r}+\frac{1}{r}\frac{\partial \overline{q_\theta q_\theta}}{\partial \theta}+\frac{\partial \overline{q_\theta q_z}}{\partial z}=$$
$$-\frac{1}{r}\frac{\partial \overline{p}}{\partial \theta}+\frac{1}{Re}\left(\frac{1}{r^2}\frac{\partial r^2\overline{\tau_{r\theta}}}{\partial r}+\frac{1}{r}\frac{\partial \overline{\tau_{\theta\theta}}}{\partial \theta}+\frac{\partial \overline{\tau_{z\theta}}}{\partial z}\right) \tag{3}$$

$$\frac{\partial \overline{q_z}}{\partial t}+\frac{1}{r}\frac{\partial \overline{q_r q_z}}{\partial r}+\frac{1}{r}\frac{\partial \overline{q_\theta q_z}}{\partial \theta}+\frac{\partial \overline{q_z q_z}}{\partial z}=$$
$$-\frac{\partial \overline{p}}{\partial z}+\frac{1}{Re}\left(\frac{1}{r}\frac{\partial r\overline{\tau_{rz}}}{\partial r}+\frac{1}{r}\frac{\partial \overline{\tau_{z\theta}}}{\partial \theta}+\frac{\partial \overline{\tau_{zz}}}{\partial z}\right) \tag{4}$$

where p is the pressure.

Eq.(1) is the continuity equation, Eqs.(2)-(4) are the momentum equations and Re the flow Reynolds number defined as $Re = U_{\text{jc}}D/\gamma$, where γ is the kinematic viscosity.

The sub-grid scale stress tensor is approximately equal to $\overline{\tau}_{ij}=(\gamma+\gamma_{\text{T}})2\overline{S_{ij}}$, where $\overline{S_{ij}}=\frac{1}{2}\left(\frac{\partial v_i}{\partial x_j}+\frac{\partial v_j}{\partial x_i}\right)$, v is the gas-phase velocity and the turbulent viscosity γ_{T} can be modeled with the standard Smagorinsky subgrid scale model:

$$\gamma_{\text{T}} \triangleq (C_{\text{s}}\varDelta)^2\,|\,\overline{S}\,| = (C_{\text{s}}\varDelta)^2\sqrt{2\overline{S}_{ij}\overline{S}_{ij}} \tag{5}$$

In which, $i, j = r,\ \theta,\ z$ in this article; the sub-grid scale $\varDelta=(r\Delta r\Delta\theta\Delta z)^{1/3}$ and C_{s} the model coefficient. The isotropic turbulence theory points out that C_{s} should be assumed to be 0.18, which is too high for the shear flow. After several trials, C_{s} is reduced to 0.1 in the final simulations, which offers satisfied outcomes.

The governing equations are discretized into a staggered-grid system with the finite difference method. The nonlinear convective terms are divided into two parts:

$$C_i=\frac{\partial \overline{q}_i\,\overline{q}_j}{\partial x_j}=\frac{1}{2}\left(\frac{\partial \overline{q}_i\,\overline{q}_j}{\partial x_j}+\overline{q}_j\frac{\partial \overline{q}_i}{\partial x_j}\right) \tag{6}$$

and discretized with the skew-symmetric scheme in order to reduce the aliasing errors, suggested by A. G. Kravchenko, et al.[10]. In the scheme, the conservative parts are discretized with the second-order central difference scheme and the non-conservative parts with the second-order three-point-upwind scheme. The liner diffusion terms are discretized with the second-order central difference scheme. The third-order explicit Runge-Kutta algorithm is adopted for the time marching.

The governing equations are solved with the fractional step projection method improved by X. Wu, et al.[11]. The Poisson equation for the pressure correction is solved with fast standard Fourier transforms in the periodic (circumferential) direction, fast cosine Fourier transforms (cosFFT) in the axial direction (see Ref.[12]) and then cyclic reduction in the radial direction, usually called Fourier analysis cyclic reduction (FACR) direction method originally proposed by R. W. Hockney[13]. The cosFFT routines can be used to solve equations with Neumann conditions at the boundaries. In the present numerical strategy, the pressure Poisson equation is specified with Neumann boundary conditions in the axial direction.

2.2. Particle-phase equations

Particles are tracked by the Lagrangian trajectory method. All particles are regarded as point-particles with the same material density ρ_{p} and the same diameter d_{p}. The interactions among particles are neglected due to the assumption of dilute flow in the present study. If only drag forces are considered, the equations describing particles' motion in cylindrical coordinates can be written for the velocity in three directions:

$$\left.\begin{aligned} \frac{\mathrm{d}v_{\mathrm{p}r}}{\mathrm{d}t} &= \frac{f(v_r - v_{\mathrm{p}r})}{\tau_{\mathrm{rp}}} + \frac{v_{\mathrm{p}\theta}^{\ 2}}{r} \\ \frac{\mathrm{d}v_{\mathrm{p}\theta}}{\mathrm{d}t} &= \frac{f(v_\theta - v_{\mathrm{p}\theta})}{\tau_{\mathrm{rp}}} - \frac{v_{\mathrm{p}r}v_{\mathrm{p}\theta}}{r} \\ \frac{\mathrm{d}v_{\mathrm{p}z}}{\mathrm{d}t} &= \frac{f(v_z - v_{\mathrm{p}z})}{\tau_{\mathrm{rp}}} + g \end{aligned}\right\} \tag{7}$$

where v_p is the velocity of particle and g the acceleration of gravity. The second terms in the right are centrifugal forces and

$$\frac{\mathrm{d}\boldsymbol{x}_\mathrm{p}}{\mathrm{d}t} = \boldsymbol{v}_\mathrm{p} \tag{8}$$

for the displacements, where f is the drag correction coefficient and according to Ref. [14], it equals

$$f = \begin{cases} 1 & Re_\mathrm{p} < 1 \\ 1 + 0.15Re_\mathrm{p}^{0.687} & 1 \le Re_\mathrm{p} < 1\,000 \\ 0.44\times\dfrac{Re_\mathrm{p}}{24} & Re_\mathrm{p} \ge 1\,000 \end{cases} \tag{9}$$

where the particle Reynolds number is defined as

$$Re_\mathrm{p} = \frac{\rho d_\mathrm{p}\left|\boldsymbol{v} - \boldsymbol{v}_\mathrm{p}\right|}{\mu}$$

where ρ is the gas density and μ the dynamic viscosity. τ_{rp} is the particle relaxation time expressed by

$$\tau_{\mathrm{rp}} = \frac{\rho_\mathrm{p} d_\mathrm{p}^{\ 2}}{18\mu}$$

In addition, the particle motions do not take the sub-grid scale fluctuations into account because the particles under study are heavy with material density three orders of magnitude larger than the air.

2.3. Boundary conditions for two phases

The jet inlet conditions are defined by

$$\left.\begin{aligned} q_z(r,\theta,0) &= q_{z0}\left(1 - \frac{2r}{D}\right) \\ \frac{\partial q_r}{\partial z} = \frac{\partial q_\theta}{\partial z} &= 0 \quad (z = 0, 0 \le r/D \le 0.5) \\ q_z(r,\theta,0) &= 0 \\ \frac{\partial q_r}{\partial z} = \frac{\partial q_\theta}{\partial z} &= 0 \quad (z = 0, 0.5 < r/D \le R_\mathrm{L}) \end{aligned}\right\} \tag{10}$$

where R_L is the computation domain in the radial direction. Hereinafter, the dash denoting the filtering operation is omitted.

To simulate the shear instability in jet, the disturbances are supposed to obey the Gaussian distribution on the axial components of the gas-phase velocity.

To the exit boundary, are applied the non-reflection conditions[2], which are defined by the following equations in the radial, circumferential and axial directions:

$$\frac{\partial q_r}{\partial t} + q_{z\mathrm{con}}\frac{\partial q_r}{\partial z} = \frac{C_1}{\rho}\left(\frac{\partial r\tau_{rr}}{\partial r} + \frac{\partial \tau_{r\theta}}{\partial \theta} - \tau_{\theta\theta}\right) \tag{11}$$

$$\frac{\partial q_\theta}{\partial t} + q_{z\mathrm{con}}\frac{\partial q_\theta}{\partial z} = \frac{C_1}{\rho}\left(\frac{1}{r^2}\frac{\partial r^2\tau_{r\theta}}{\partial r} + \frac{1}{r}\frac{\partial \tau_{\theta\theta}}{\partial \theta}\right) \tag{12}$$

$$\frac{\partial q_z}{\partial t} + q_{z\mathrm{con}}\frac{\partial q_z}{\partial z} = \frac{C_1}{\rho}\left[\frac{1}{r}\frac{\partial r\tau_{rz}}{\partial r} + \frac{1}{r}\frac{\partial \tau_{z\theta}}{\partial \theta} - \mu\left(\frac{1}{r}\frac{\partial}{\partial r}\left(\frac{\partial q_r}{\partial z}\right) - \frac{1}{r}\frac{\partial q_\theta}{\partial z}\right)\right] \tag{13}$$

where $q_{z\mathrm{con}}$ is the averaged transport velocity of large scale eddies, assumably 0.3 of the averaged axial velocity and C_1 a relative viscosity coefficient, assumed to be 0.8.

In the radial direction, the following open outflow boundary conditions are specified to match the pressure gradient in that direction:

$$\left.\begin{aligned} \frac{1}{r}\frac{\partial}{\partial r}\left(\frac{q_r q_r}{r}\right) &= -\frac{\partial p}{\partial r} \\ \frac{\partial q_\theta}{\partial r} = \frac{\partial q_z}{\partial r} &= 0 \quad (r/D = R_\mathrm{L}) \end{aligned}\right\} \tag{14}$$

In the circumferential direction, the periodic boundary condition is adopted and the velocity transform variables are

$$q_i\big|_{\theta=0} = q_i\big|_{\theta=2\pi} \tag{15}$$

2.4. Two-way coupling model

As presented in Section 2.3, the continuous phase carries particles with the help of the drag force mainly in the ith direction:

$$F_{\mathrm{d}i} = \frac{fm_\mathrm{p}(v_i - v_{\mathrm{p}i})}{\tau_{\mathrm{rp}}}$$

where m_p is the particle mass and $m_\mathrm{p} = 4\rho_\mathrm{p}\,\pi\, d_\mathrm{p}^3/3$.

Assuming that there are totally n_p particles in one of the cells to be computed, the reaction between the particle-phase and the fluid-phase is then embodied in the source terms added to the following fluid-phase momentum equation:

$$S_{\mathrm{p}i} = -\frac{1}{\rho\Delta V}\sum_{k=1}^{n_\mathrm{p}} F_{\mathrm{d}i}^k = -\frac{1}{\rho\Delta V}\sum_{k=1}^{n_\mathrm{p}}\frac{fm_\mathrm{p}(v_i^k - v_{\mathrm{p}i}^k)}{\tau_{\mathrm{rp}}} \tag{16}$$

where ΔV is the volume of the cell to be computed. The source terms represent the reaction of all particles to the fluid phase in that cell.

By applying the filtering function to Eq.(16), the source terms become

$$S_{\mathrm{p}i} = -\frac{F}{\Delta V}\left[\overline{n}_\mathrm{p}(\overline{v}_i - \overline{v}_{\mathrm{p}i}) + (\overline{n'_\mathrm{p}v'_i} - \overline{n'_\mathrm{p}v'_{\mathrm{p}i}})\right] \tag{17}$$

where $F = 3\pi\mu\, d_{\mathrm{p}} f/\rho$, $\bar{n}_{\mathrm{p}}$ is the mean number of particles, n'_{p} the fluctuating particle number and v'_i and $v'_{\mathrm{p}i}$ are the sub-grid scale fluctuating velocity of the fluid-phase and that of the particle-phase. Therefore, $\overline{n'_{\mathrm{p}} v'_i}$ and $\overline{n'_{\mathrm{p}} v'_{\mathrm{p}i}}$ are correlation terms of the particle number and the fluctuating velocity.

Now a gradient analogy model is applied to each of the terms:

$$\overline{n'_{\mathrm{p}} v'_i} = -\gamma_{\mathrm{TS}} \frac{\partial \bar{n}_{\mathrm{p}}}{\partial x_i} \tag{18}$$

$$\overline{n'_{\mathrm{p}} v'_{\mathrm{p}i}} = -\gamma_{\mathrm{TP}} \frac{\partial \bar{n}_{\mathrm{p}}}{\partial x_i} \tag{19}$$

where γ_{TS} is the scalar diffusivity coefficient in terms of the Schmidt number Sc and the turbulent viscosity γ_{T} which is defined as

$$\gamma_{\mathrm{TS}} = \frac{\gamma_{\mathrm{T}}}{Sc} \tag{20}$$

In which γ_{TP} is the particle-phase turbulent diffusivity coefficient defined by[7]

$$\gamma_{\mathrm{TP}} = \frac{f T_{\mathrm{Li}}}{f T_{\mathrm{Li}} + \tau_{\mathrm{rp}}} \gamma_{\mathrm{T}} \tag{21}$$

where T_{Li} is the Lagrangian relaxation time, assumed to be

$$T_{\mathrm{Li}} = \frac{\alpha}{C_{\varepsilon}^{2/3} C_{\mathrm{v}}^{1/2} \sqrt{2/3}\,|\bar{S}|} \tag{22}$$

where $\alpha = 0.165$, $C_{\mathrm{v}} = 0.05$ and $C_{\varepsilon} = 1.0$.

3. Results

A jet with a flow Reynolds number of 2 400 is simulated in the present study. Table 1 lists the particle parameters selected in studying the particles' backward modulation of the near-field dynamics.

Table 1 Simulation parameters

Parameter	Value
Fluid density/(kg·m^{-3})	1.19
Particle density/(kg·m^{-3})	2 500
Nozzle diameter/(kg·m^{-3})	0.04
Particle diameter/μm	110
Jet velocity/(m·s^{-1})	0.88
Particle inlet velocity/(m·s^{-1})	0.73
Particle Stokes number	2.11
Mass loading ratio/%	<5
Dynamics viscosity/(kg·m^{-1}·s^{-1})	1.75×10^{-5}

3.1. *Effects of near-field vortex dynamics—two-way coupling between particles*

Fig.1 shows the contour of Ω_{φ} at an instant in the near-fields of jets. The circumferential component of vorticity is defined as

$$\Omega_{\varphi} = \frac{1}{r}\frac{\partial r u_z}{\partial r} - \frac{1}{r}\frac{\partial u_r}{\partial \varphi} \tag{23}$$

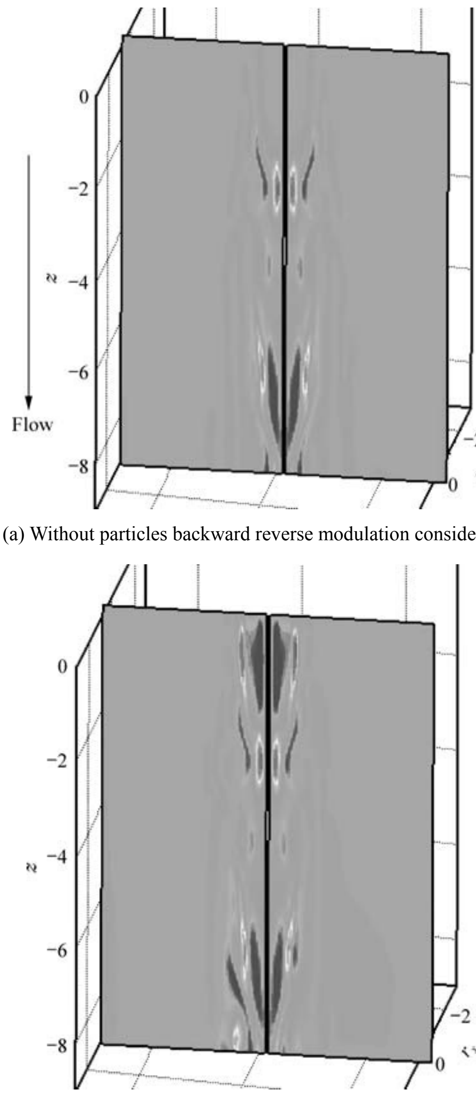

(a) Without particles backward reverse modulation considered

(b) With particles backward reverse modulation considered

Fig.1 A contour of vorticity components in circumferential direction in near-fields.

It is observed that the vortex rings are the main flow structures in the near-fields. The breakup of vortex rings to form streamwise vortices leads to conversion into far-field turbulence. The numerical simulation results are in agreement with the experimental observation[15].

In the case of the single-phase flow without particles, the vortex rings appear at the position z/D=2. However, when laden with particles, the jet instability earlier excited by the particles makes the vortex rings appear closer to the jet nozzle exit as a result of the laden particles accelerating the transition in the near-fields.

Fig.2 shows the particle dispersion in the near-field vortex represented by the vorticity contour, where the black dots indicate the particles.

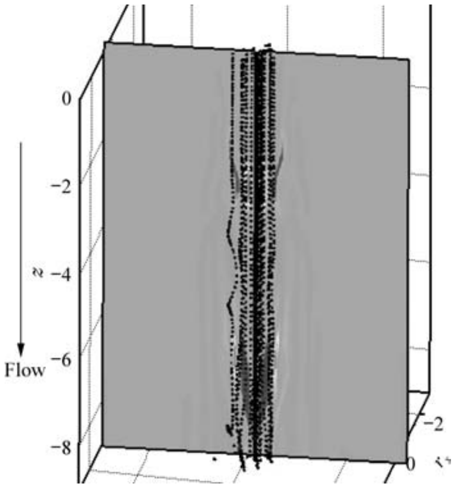

(a) Without particles backward reverse modulation

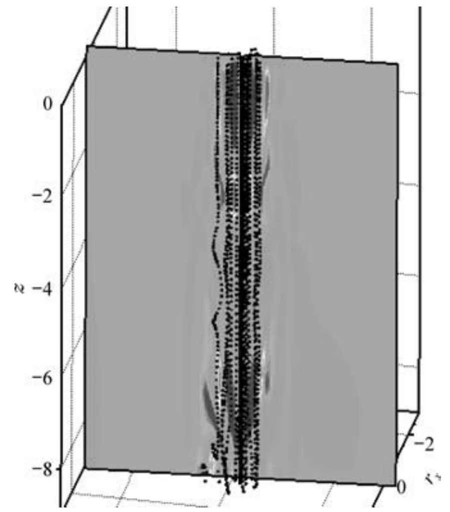

(b) With particles reverse backward modulation considered

Fig.2 Particles dispersion in near-field vortex.

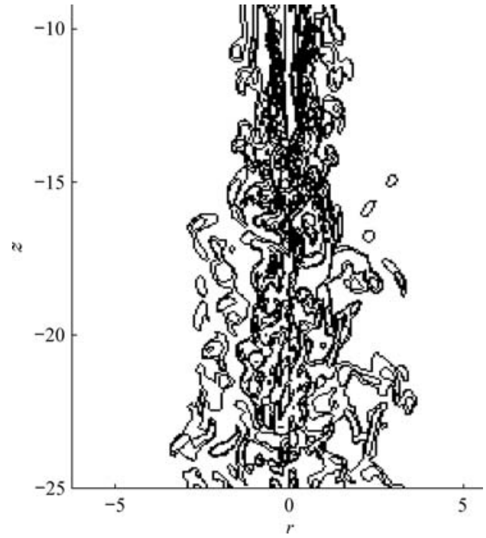

(a) Contour of turbulent vortices

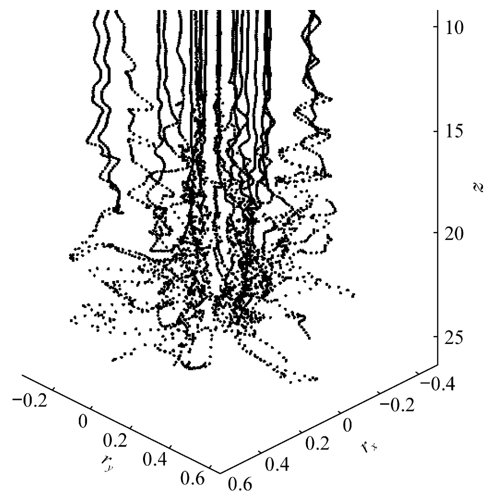

(b) Particles scattering pattern

Fig.3 Turbulence and particles dispersion in far-fields.

From Fig.2, it can be seen that particles almost move downwards in their initial momentum direction until z/D=2. The particles downstream in the shear layer between the jet's core fluid and the ambient fluid move in spiral trajectories; by contrast, the particles in the jet's core still move along nearly straight paths. There seems to be hardly any distinct difference between the cases with and without particle coupling modulation at z/D=0-5, just meaning at the jet's core.

The particles under study belong to those having moderate inertia. Therefore, their dispersion is determined by both the flow structures and their own inertia. In the near-fields, the initial streamwise vortices are not strong enough to disperse the particles to the outer edges. Compared with the particles scattering pattern in the far-fields in Fig.3, where the particles having moderate inertia are more dispersed, it can be discovered that the turbulent diffusion or the extension of turbulent coherent structures results in wider particle dispersion. The spiral paths of the particles outside the jet's core also reflect the instability of jet flow.

The development of two-phase jet is determined by the formation of flow structure and particle's reverse backward modulation in the near-fields. To further demonstrate modification of the initial jet structure by particles, Fig.4 shows the isosurfaces of the vorticity in the circumferential direction at an instant. With the particle reverse backward modulation, the vortex rings appear closer to the jet nozzle exit than the case without particle modulation. It can thus be concluded that it is the laden particles that excite the instability of jet. This accords with the experimental observations and measured data[16-17]. The earlier breakup of vortex rings is observed at the downstream of the particle-laden jets. Because of the earlier breakup of vortex rings caused by the jet laden with particles having inertia, the streamwise structures would appear (see Figs.4(b), (d), (f), (g)). This is helpful to explain why particles in the near-fields increase the flow fluctuating intensity of flows observed in the earlier experiments[16-17].

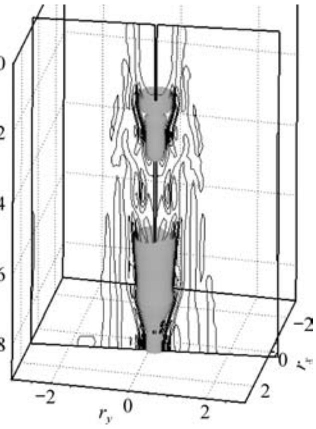

(a) $\Omega_\varphi = 0.25$ without particles two-way coupling

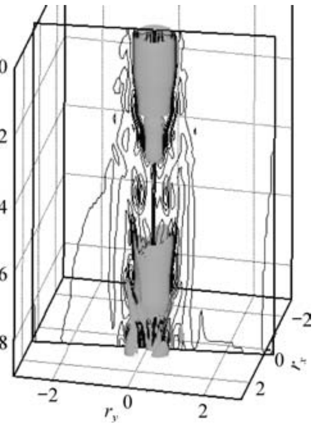

(b) $\Omega_\varphi = 0.25$ with particles two-way coupling

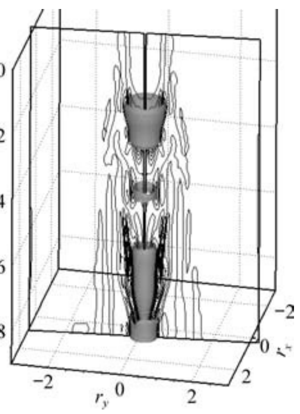

(c) $\Omega_\varphi = -0.25$ without particles two-way coupling

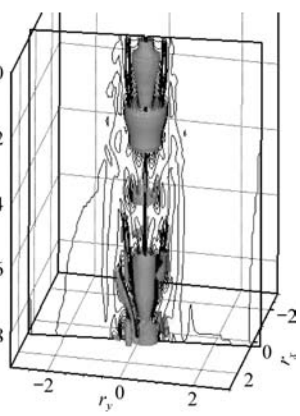

(d) $\Omega_\varphi = -0.25$ with particles two-way coupling

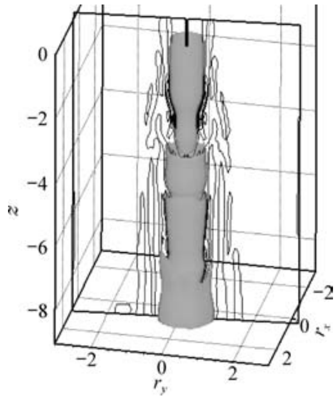

(e) Ω_φ=0.50 without particles two-way coupling

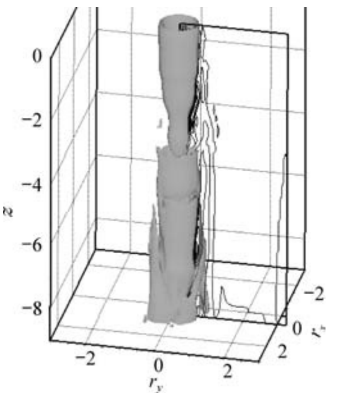

(f) $\Omega_\varphi = 0.50$ with particles two-way coupling

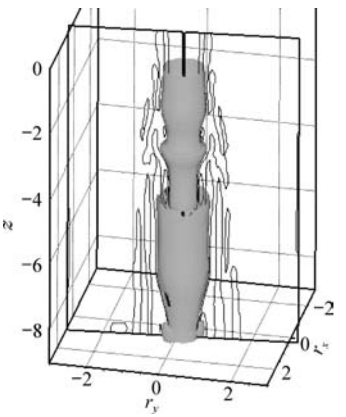

(g) Ω_φ=–0.50 without particles two-way coupling

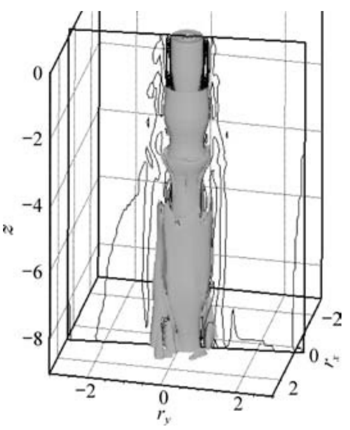

(h) $\Omega_\varphi = -0.50$ with particles two-way coupling

Fig.4 Isosurface of vorticity component in circumferential direction in near-fields.

3.2. *Near-field statistical properties—two-way coupling effects of particles*

Fig.5 shows the two-phase mean velocity components without particle reverse backward modulation. From Fig.5, the abscissa denotes non-dimensional velocity similarity variables $\eta = r/(z-z_0)$, where z is the axial displacement from the nozzle exit and z_0 the virtual original point, taken as 4.4 in the present study. It can be seen that in the near-fields, the profiles of two-phase velocity components in different sections do not have the self-similarity and the axial velocity strongly diffuses. This is quite different from the far-fields of the jet which possesses the property of holding self-similarity.

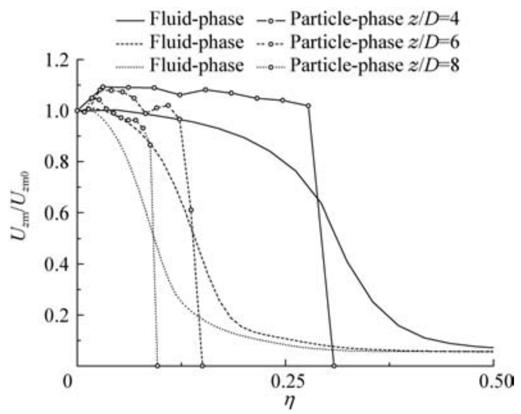

Fig.5　Two-phase mean velocity components in axial direction in near-fields.

Figs.6-7 show the two-way coupling effects of particles on the near-field statistical properties. In them, the abscissa is defined by

$$\xi = r / r_{0.5}$$

where $r_{0.5}$ is the half width of the jet.

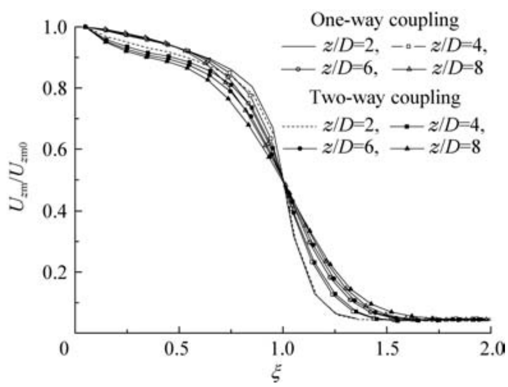

Fig.6　Gas-phase mean velocity components in axial direction.

Particles change the diffusion of the mean axial velocity in the radial direction. The particles decrease the mean velocity when $\xi<1$, while increase when $\xi>1$.

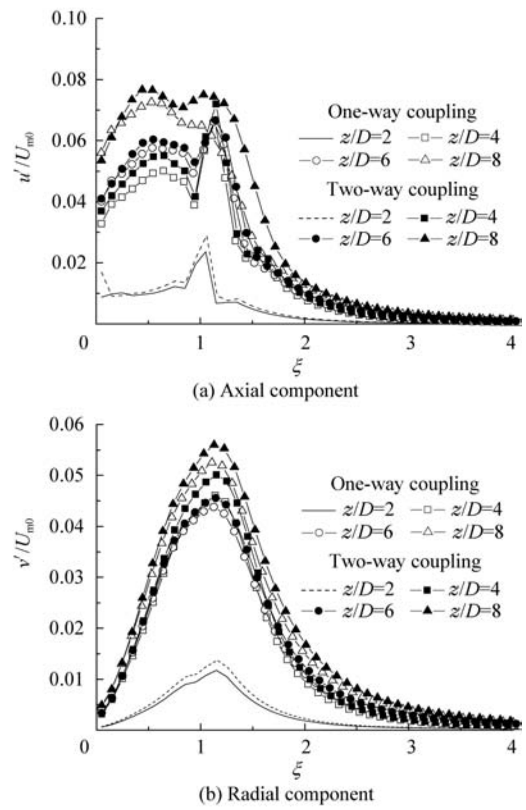

Fig.7　Gas-phase root mean square velocities.

It is discovered that the turbulence intensity increases as the flow develops. When the jet is laden with particles, the turbulence intensity in different sections is larger than that when not laden with particles. From Fig.4, the jet instability has been induced by particles earlier and hence the initial vortex rings are broken up. Therefore, particles strengthen the turbulence intensity.

Fig.8 shows the increase in axial components of turbulence fluctuation along the axial central line. It is shown that in the initial state of the jet, the axial flow fluctuating intensity increases; whereas in the far-fields (commonly in the fields at z/D>8-10 in the present study) the axial turbulence along the central line decreases. The modulation of flow by particles depends on the jet location.

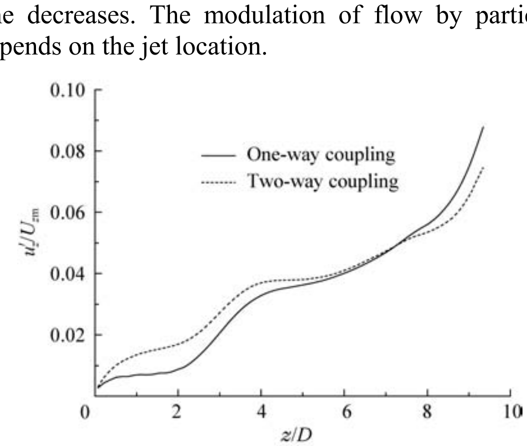

Fig.8　Increase in gas-phase axial turbulence fluctuation along axial central line.

The different states of development generate the different flow structures thereby changing the mode of particles' interaction with the structures. In the initial state, particles mainly excite the flow instability, acting as significant disturbances in the flow fields. In the far-fields, they mainly function as energy sinks to filter the high frequency turbulence fluctuation thus depressing the turbulence intensity.

Due to their own inertia, particles are in position to respond to the turbulence eddies only when their characteristic time is longer than the particle relaxation time. The turbulence fluctuations with the characteristic time shorter than particles' relaxation time are then screened. Consequently, the gas-phase flow intensity slims down in the fully developed two-phase turbulence. For more information about the mechanism of particle modulation of turbulence, refer to Ref.[18].

4. Conclusions

This article has studied the near-field dynamics in a particle-laden round turbulent jet. The gas-phase turbulent flow is modeled in a large-eddy simulation in cylindrical coordinates. The discrete particles are tracked by the Lagrangian trajectory model. The point-force model adopted as a two-way coupling model is employed in the simulation.

The simulation results of statistical velocities and flow structures reveal the effects of particle modulation. The changes in mean and r.m.s velocity are evidenced to be caused by the flow structures modulated by particles. Particles mainly excite the initial instability of the jet and bring about the earlier breakup of vortex rings in the near-fields, resulting in increases in flow fluctuating intensity in the axial and radial directions. The mean velocity modulated by particles is different from each other according to where it is; for instance, in the jet core, it decreases while outside it increases.

References

[1] Verzicco R, Orlandi P. Direct simulations of the transitional regime of a circular jet. Physics of Fluids 1994; 6 (2): 751-759.

[2] Dai Y, Kobayashi T, Taniguchi N. Large eddy simulation of plane turbulent jet flow using a new outflow velocity boundary condition. JSME International Journal, Series B: Fluids and Thermal Engineering 1994; 37(2): 242-253.

[3] Olsson M, Fuchs L. Large eddy simulation of the proximal region of a spatially developing circular jet. Physics of Fluids 1996; 8(8): 2125-2137.

[4] Fan Q L. Study on coherent structures of two-phase round jets. PhD thesis, Department of Engineering Mechanics, Tsinghua University, 2000. [in Chinese]

[5] Fan Q L, Zhang H Q, Guo Y C, et al. Experimental studies on two-phase round turbulent jet coherent structures. Tsinghua Science and Technology 2000; 5(1): 105-108.

[6] Yuu S, Ikeda K, Umekage T. Flow-field prediction and experimental verification of low Reynolds number gas-particle turbulent jets. Colloids and Surfaces A: Physicochemical and Engineering Aspects 1996; 109: 13-27.

[7] Yuu S, Ueno T, Umekage T. Numerical simulation of the high Reynolds number slit nozzle gas-particle jet using subgrid-scale coupling large eddy simulation. Chemical Engineering Science 2001; 56(14): 4293-4307.

[8] Luo K, Jin J, Zheng Y Q, et al. Direct numerical simulation of particle dispersion in gas-solid compressible turbulent jets. Chinese Journal of Chemical Engineering 2005; 13(2): 161-166.

[9] Rong Y. Two-way coupling large eddy simulation of two-phase particle-laden round jets. PhD thesis, School of Aerospace, Tsinghua University, 2006. [in Chinese].

[10] Kravchenko A G, Moin P. On the effect of numerical errors in large eddy simulations of turbulent flows. Journal of Computational Physics 1997; 131(2): 310-322.

[11] Wu X, Squires K D, Wang Q. Extension of the fractional step method to general curvilinear coordinate systems. Numerical Heat Transfer, B-Fundamental 1995, 27(2): 175-194.

[12] Orlandi P. Fluid flow phenomena. Dordrecht, Netherlands: Kluwer Academic Publishers, 2000; 24-33.

[13] Hockney R W. The potential calculation and some applications. Methods in Computational Physics, Plasma Physics 1970; 9: 135-211.

[14] Putnam A. Integrable form of droplet drag coefficient. American Rocket Society Journal 1961; 31:1467-1468.

[15] Suprayan R, Fiedler H E. On streamwise vortical structures in the near-field of axisymmetric shear layers. Mechanica 1994; 29(4): 403-410.

[16] Rong Y, Cui J L, Zhang H Q, et al. Experimental investigation of particle-laden two-phase round jet. Proceedings of the 5th International Symposium on Coal Combustion. 2003; 83-86.

[17] Cui J L, Zhang H Q, Wang B, et al. Flow visualization and laser measurement on particle modulation to gas-phase turbulence. Journal of Visualization 2006; 9(3): 339-345.

[18] Wang B, Zhang H Q, Liu Y, et al. Particle modulations to turbulence in two-phase round jets. Acta Mechanica Sinica 2009; 25(5): 611-617.

Biography:

Wang Bing Born in 1977, he received B.S. and Ph.D. degrees from Tsinghua University in 2000 and 2005 respectively, and then became a teacher there. His main research interests are power and propulsion technology, multi-phase flow dynamics and combustion.
E-mail: wbing@tsinghua.edu.cn